Conformational Changes in the Extrinsic Manganese Stabilizing Protein Can Occur upon Binding to the Photosystem II Reaction Center: An Isotope Editing and FT-IR Study†

Ronald S. Hutchison,‡ Scott D. Betts,§,|| Charles F. Yocum,§ and Bridgette A. Barry*,‡

Department of Biochemistry, College of Biological Sciences, University of Minnesota, St. Paul, Minnesota 55108, and Departments of Chemistry and Biology, The University of Michigan, Ann Arbor, Michigan 48109

Received October 2, 1997; Revised Manuscript Received November 25, 1997

ABSTRACT: Photosystem II catalyzes the light-driven oxidation of water and reduction of plastoquinone in oxygenic photosynthesis. The manganese stabilizing protein (MSP) of photosystem II is an extrinsic subunit that plays an important role in catalytic activity. This subunit can be extracted and re-bound to the photosystem II reaction center. Extraction is associated with decreased stability of manganese binding by the enzyme and by loss in high rates of oxygen evolution activity; reconstitution reverses these phenomena. Since little is known about the assembly of complex membrane proteins, we have employed isotope editing and vibrational spectroscopy to obtain information about any changes in secondary structure that occur in MSP upon functional reconstitution to photosystem II. The spectroscopic data obtained are consistent with substantial changes in conformation when MSP binds to photosystem II; approximately 30−40% of the peptide backbone undergoes a change in secondary structure. These conclusions were reached by comparing different aliquots, before and after binding, of the same ^{13}[C]MSP sample. Analysis of amide I band line shapes through Fourier deconvolution and nonlinear regression suggests that binding of MSP to photosystem II is associated with a decrease in random structure and an increase in β-sheet content. We conclude that binding of MSP to the reaction center can induce folding of MSP. Our results also indicate that, in solution, MSP can sample a variety of conformational states, which differ in hydrogen bonding of the peptide backbone.

Oxygenic photosynthesis employs two reaction centers for the light-driven transfer of electrons from water to $NADP^+$ and generates the electrochemical gradient that can be used in the synthesis of ATP. Photosystem II (PSII)[1] is the multisubunit protein complex that uses light energy to oxidize water and form molecular oxygen with a concomitant reduction of plastoquinone to plastoquinol. The active site of water oxidation in PSII contains four manganese atoms and accumulates the four oxidizing equivalents that are necessary to produce molecular oxygen. These sequentially oxidized forms of the catalytic site are called the S states. The minimum size of an oxygen-evolving PSII reaction center is at least eight protein subunits (reviewed in refs *1* and *2*).

Photosystem II contains several extrinsic subunits that play important roles in stabilizing the active site. One of these, the nuclear-encoded manganese stabilizing protein (MSP), has a molecular mass of approximately 26 kDa (*3*) and is synthesized with a transit sequence that targets the protein to the thylakoid lumen (reviewed in ref *4*). Immunological techniques have shown that there are two copies of the MSP subunit per PSII reaction center (*5*); the dissociation constant has been measured to be <1 to 12 nM (*6, 7*). MSP has been deleted by genetic methods in cyanobacteria and in green algae. In cyanobacteria, strains in which the MSP has been deleted can grow photoautotrophically, but they evolve oxygen at lower rates and are more sensitive to photoinhibition (*8*−*12*). In green algae, on the other hand, a strain in which MSP has been deleted cannot grow photoautotrophically (*13*).

MSP can be removed from the plant PSII reaction center by treatment of samples with high concentrations of Tris, $CaCl_2$, or with urea plus NaCl (2.6 M/200 mM) (*14*−*17*). Once released from the reaction center, MSP behaves as a water-soluble, hydrophilic protein and can be re-bound to the PSII reaction center (*18*). After removal of MSP by urea or $CaCl_2$ treatments, the steady-state rate of oxygen evolution is slower (*19*), and PSII is more susceptible to photodamage, showing instability in oxygen evolution under prolonged illumination (*20*). At low chloride concentrations, two of the four manganese atoms are easily lost from the reaction

† Supported by NSF MCB 94-18164 (B.A.B.) and by NSF MCB 93-14743 (C.F.Y.).

* Corresponding author: 140 Gortner Laboratory, Department of Biochemistry, College of Biological Sciences, University of Minnesota, St. Paul, MN. Phone: 612-624-6732. Fax: 612-625-5780. E-mail: barry@biosci.cbs.umn.edu.

‡ University of Minnesota.

§ University of Michigan.

|| Current address: Department of Biology, Massachusetts Institute of Technology, Cambridge, MA 02139.

[1] Abbreviations: CD, circular dichroism; BSA, bovine serum albumin; Chl, chlorophyll; DCBQ, 2,6-dichlorobenzoquinone; FT-IR, Fourier transform infrared spectroscopy; *K*, resolution enhancement factor; MSP, manganese stabilizing protein; MES, 2-(*N*-morpholino)-ethanesulfonic acid; PSII, photosystem II; SDS−PAGE, sodium dodecyl sulfate−polyacrylamide gel electrophoresis.

S0006-2960(97)02446-X CCC: $15.00 © 1998 American Chemical Society
Published on Web 04/01/1998

center in the absence of MSP; this loss results in inactivation of the enzyme (*17, 21*). Perturbations in the oxidation potentials of the S states are also observed upon removal of MSP (*22*−*24, 12*). Previous work has shown that the precursor form of MSP can be expressed in *Escherichia coli*, where it is correctly processed and exported into the periplasmic space. The overexpressed protein has been purified and re-bound to PSII (*25, 20*). Bacterially expressed recombinant MSP is functionally indistinguishable from protein extracted from PSII; that is, after reconstitution, oxygen evolution rates are increased, and the enzyme is stable under illumination (*20, 25*). Recombinant MSP binds to PSII with the same stoichiometry as the native protein (*20, 25*).

We have used isotope editing to obtain more information about the role of MSP in PSII. This technique provides an opportunity to follow conformational changes in MSP, even on the unlabeled background of the PSII reaction center, through the use of spectroscopic techniques that are sensitive to isotopic composition. To implement this technique, an *E. coli* strain expressing MSP was grown on minimal media. Cultures were provided either [^{12}C]glucose or [^{13}C]glucose. As expected, use of [^{13}C]glucose as a carbon source resulted in uniform ^{13}C labeling of the expressed protein (*26, 27*). This uniformly ^{13}C labeled MSP or the ^{12}C control MSP was then re-bound to plant PSII membranes (*28*) that had been depleted of the native protein, but not of manganese (*20*). To ensure that all bound [^{12}C]- or [^{13}C]MSP was specifically associated with a high affinity binding site, PSII membranes were then treated with detergent, and ion-exchange chromatography was performed. This procedure yields PSII complexes that have been depleted of nonessential antenna proteins (*29*).

Fourier-transform infrared spectroscopy (FT-IR) has proven to be a useful technique with which to analyze the structure of proteins and to follow structural changes in proteins (reviewed in refs *30* and *31*). This technique is sensitive to isotopic composition. Uniform ^{13}C labeling of proteins results in an overall downshift of the amide I bands by approximately 45−55 cm^{-1}, allowing the ^{13}C-labeled subunits to be distinguished from other, unlabeled proteins (*26, 27*). The amide I vibration arises primarily from the C═O vibration of the peptide backbone, and the frequency of this band is sensitive to changes in hydrogen bonding and in transition dipole coupling (*32*). The frequency and line shape of the amide I band have been used to predict secondary structure; several different methods of analysis have been employed (for example, see refs *33*−*39*). The advantages and disadvantages of these methods have been reviewed (*30, 31*).

While FT-IR and amide I band analysis have been applied to MSP in solution, the reported spectra of MSP are quite different from each other (*40*−*43*). Our own FT-IR studies of MSP in solution (presented herein) have led us to develop the hypothesis that MSP has an undefined structure in solution and that substantial changes in secondary structure must accompany the rebinding of this subunit to PSII. In this communication, we present evidence from FT-IR spectroscopy that reconstitutively active forms of MSP possess different solution structures. We also show that the structure of MSP can be substantially altered upon functional reconstitution to PSII.

MATERIALS AND METHODS

Purification of MSP. *E. coli* containing the *psb*O expression plasmid (*20*) was grown on M9 minimal media supplemented with 1 mM $CaCl_2$ and 0.2 mM $MgSO_4$, according to a method previously described (*26, 27*). The host strain was BL21(DE3)pLysS(F^- *ompT* r_B^- *mB*$^-$). The *psb*O gene employed has been engineered to replace the amino-terminal transit sequence with a methionine residue. This mutation (Met-MSP) induces modified binding of MSP to PSII, but only at low temperature; binding and activity at room temperature are similar to those obtained with wild-type protein (*75*). The advantage of the use of Met-MSP is that expression of high yields of isotopically labeled protein does not depend on processing. The glucose concentration was 2 g/L, and either [^{12}C]glucose or [^{13}C]glucose (99% $^{13}C_6$, Isotec, Miamisburg, OH) was employed. This procedure yielded [^{12}C]MSP or [^{13}C]MSP, respectively. To grow cultures on minimal media, 20 mL of an overnight culture (in minimal media) was introduced into 1 L of minimal media and grown until the OD_{600} was 0.4 (approximately 4 h). The culture was then induced with 40 μM IPTG and was grown for an additional 4 h. Purification of the MSP was carried out using two rounds of ion-exchange chromatography as described (*44, 45*), but with the following changes: betaine was omitted from solutions for column chromatography, and the first column was a low-pressure, 25-mL Fast-flow Q column (Pharmacia, Uppsala, Sweden).

Purification of MSP from spinach PSII membranes (*28*) was performed as described (*46*). PSII membranes were treated for 30 min with a buffer containing 2 M NaCl, 50 mM MES−NaOH (pH 6.0), and 0.4 M sucrose to remove the 18- and 24-kDa proteins (*20, 47*). After centrifugation at 48000*g* for 30 min, the pellet was resuspended in 50 mM MES−NaOH (pH 6.0) and 0.4 M sucrose. The solution also contained a final concentration of either 2.6 M urea/200 mM NaCl or 1 M $CaCl_2$. This treatment released MSP from the 18- and 24-kDa-depleted PSII membranes, which were pelleted again. The supernatant, which contained MSP, was dialyzed and then loaded onto a DEAE anion-exchange column for purification (*46*). Purified MSP was exchanged into a D_2O buffer containing 5 mM MES−NaOD (p^{2}D 6.0) by concentration using a Centricon-10 (Amicon, Beverly, MA). The pD is reported as the uncorrected meter reading (*48*).

Amino-terminal sequencing confirmed both the presence of a N-terminal methionine on the *E. coli* expressed protein and the presence of the correct amino-terminal sequence in spinach (urea-released) MSP (*3*). Estimates from amino acid sequencing and composition analysis indicated that the purities of the *E. coli* derived and the urea-released spinach-derived proteins were greater than approximately 90%.

Isotope incorporation into MSP isolated from bacteria grown on [^{13}C]glucose was tested using gas chromatography/mass spectrometry on seven different *tert*-butyldimethylsilyl-derivatized amino acids from an acid-hydrolyzed MSP sample (*49*). This analysis demonstrated that greater than 95% of the carbon atoms in the MSP sample were ^{13}C. A Kratos MS-25 GC/MS equipped with a 15 m × 0.25 mm

0.25 mM film DB-1 column was employed (J&W Scientific, Folsom, CA).

Rebinding of MSP. Spinach PSII membranes (*28*) were treated with a buffer containing 2 M NaCl, 50 mM MES−NaOH (pH 6.0) and 0.4 M sucrose for 30 min to remove the 18- and 24-kDa proteins (*47, 20*). After centrifugation at 48000*g* for 30 min, the pellet was resuspended in a buffer containing 200 mM NaCl, 50 mM MES−NaOH (pH 6.0), and 0.4 M sucrose. Urea was added from a concentrated stock to give a final concentration of 2.6 M. This treatment has been shown to remove MSP while preserving the Mn-containing catalytic site (*17*). This solution was incubated in the dark for 30 min, and the sample was centrifuged at 48000*g* for 15 min. The pellet was homogenized with 12 mL of a buffer containing 0.4 M sucrose, 50 mM MES−NaOH (pH 6.0), and 60 mM NaCl and pelleted at 48000*g* for 15 min. The urea-washed PSII membranes were then resuspended to approximately 2 mg of Chl/mL, and the chlorophyll concentration was determined (*50*).

[^{12}C]- or [^{13}C]MSP was re-bound to the urea-washed PSII membranes (0.2 mg/mL Chl, 0.8 μM PSII reaction centers) in a buffer containing 60 mM NaCl, 50 mM MES−NaOH (pH 6.0), 0.4 M sucrose, 20 mM $CaCl_2$, 3.5 μM MSP, and 333 μg/mL BSA. The reaction mixture was incubated on ice for 30 min and then incubated at 20 °C for 1 h. Oxygen evolution assays were performed as described (*51*) on a Clark-type O_2 electrode (YSI 5300, YSI Inc., Yellow Springs, OH) using 10 μg/mL Chl, 400 μM recrystallized DCBQ, and 1 mM potassium ferricyanide. The concentration of MSP in solution was determined using the ultraviolet extinction coefficient previously reported, 16 mM^{-1} cm^{-1} (*46, 52*).

After reconstitution of MSP into PSII membranes, PSII complexes were purified from this material through the use of ion-exchange chromatography (*29*). PSII complexes were exchanged into a D_2O buffer containing 5 mM MES−NaOD (pD 6.0) and 0.05% *N*-dodecyl β-D-maltoside (Anatrace, Maumee, OH) through the use of a Centricon-100 (Amicon, Beverly, MA). Samples were analyzed using a modified Neville SDS−PAGE method described previously (*53*). Western analysis was performed with anti-MSP rabbit antibody, a protein A−alkaline phosphatase conjugate, and methods previously described (*54*).

FT-IR Analysis. Infrared spectra were recorded on a Nicolet Magna II-550 FT-IR spectrometer equipped with a liquid nitrogen-cooled MCT/A detector and a KBr beam splitter. The mirror velocity was 2.53 cm s^{-1}, the spectral resolution was 2 cm^{-1}, and 2000 mirror scans were co-added for each double-sided interferogram. A Happ-Ganzel apodization function and one additional level of zero-filling were employed. The sample (6 μL) was placed between two 19-mm CaF_2 windows (Harrick Scientific, Ossining, NY) using a 6-μm spacer. A Harrick temperature control cell and a recirculating water bath were used to control the temperature to ±1.0 °C. The temperature during data acquisition was 20 °C. The protein concentration for infrared studies of MSP in solution was 90−580 μM; the chlorophyll concentration for PSII samples was 37−55 mg/mL.

For data on MSP in solution, a buffer spectrum was recorded, and this spectrum was subtracted from protein spectra recorded on the same day. Comparison of [^{12}C]MSP and [^{13}C]MSP reconstituted photosytem II complexes was performed before buffer subtraction and through the use of an internal standard consisting of a solution of potassium ferricyanide (2 mM) and potassium ferrocyanide (2 mM). The 2030 cm^{-1} C≡N stretching vibration of ferrocyanide was used to correct for any small changes in path length; PSII has no infrared absorbance in the 2030 cm^{-1} region. The amplitude of the CN stretch was chosen to be approximately equal to the intensity of the amide I band of the ^{13}C-labeled MSP after reconstitution. Use of the internal standard is important in controlling for small changes in path length, which can occur in the Harrick sample cell. Use of an equimolar ferricyanide/ferrocyanide mixture at a concentration of 4 mM should provide an effective redox buffer for the PSII samples. However, as an additional precaution, samples were maintained in the dark after addition of the ferricyanide/ferrocyanide mixture. This procedure will prevent light-induced electron-transfer reactions, which could slightly alter the relative concentrations of ferricyanide and ferrocyanide. Note that the overall intensity of the amide I and amide II bands was always less than 0.7 absorbance unit.

Fourier deconvolution and second-derivative analysis were performed using Nicolet Omnic software. The parameters for deconvolution were chosen according to established procedures (*55, 56*); the *K* value was 2, the line width was 40 cm^{-1}, and the apodization function for Fourier self-deconvolution was a modified Happ-Ganzel function. Estimates of the line width were taken from the basis spectra derived previously (*33*). Grams (Galactic Industries Co., Salem, NH) was used to perform the regression analysis using spectral components with Gaussian band shapes (for example, see ref *57*). In a series of control experiments, FT-IR spectra were obtained and analyzed for the proteins myoglobin, immunoglobin G, and lysozyme. The procedures employed were shown to reproduce previous results in the literature (for example, see refs *33, 55,* and *56*).

RESULTS

Oxygen evolution measurements were performed on PSII preparations before and after reconstitution with ^{12}C- and ^{13}C-labeled MSP, as described in Materials and Methods. Since treatments to remove MSP from PSII membranes also remove the 24- and 18-kDa subunits, MSP-reconstituted samples lack the 24- and 18-kDa proteins and depend on calcium chloride for activity. PSII membranes depleted of the 24- and 18-kDa subunits exhibited control oxygen evolution rates of 660 ± 140 μmol of O_2 (mg of Chl)$^{-1}$ h^{-1} (average of 6 measurements). As previously reported (*19*), removal of MSP slows the steady-state rate of oxygen evolution to 330 ± 50 μmol of O_2 (mg of Chl)$^{-1}$ h^{-1} (average of 6 measurements). Rebinding of [^{12}C]MSP and [^{13}C]MSP, derived from expression in *E. coli*, restored oxygen rates to 530 ± 120 (average of 6 measurements) and 510 ± 100 μmol of O_2 (mg of Chl)$^{-1}$ h^{-1} (average of 6 measurements), respectively.

When [^{12}C]- or [^{13}C]MSP reconstituted PSII membranes were treated with a nonionic detergent and the monodisperse mixture was subjected to ion-exchange chromatography (*29*), the resulting PSII complexes showed the expected increase in oxygen evolution rates, as nonessential chlorophyll-containing antenna proteins were depleted (*29*). The rates were 890 ± 20 μmol of O_2 (mg of Chl)$^{-1}$ h^{-1} (average of 3

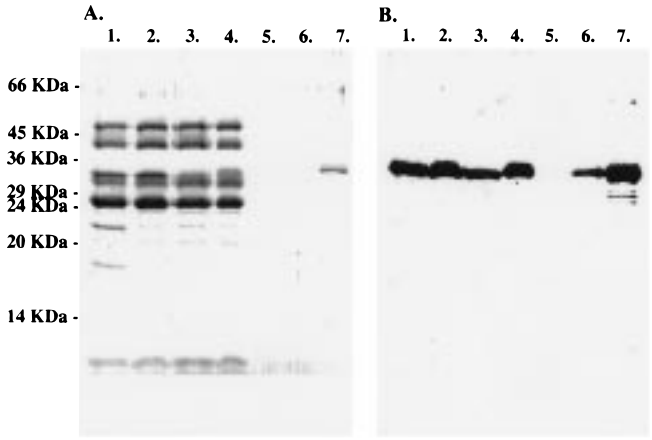

FIGURE 1: SDS−PAGE (A) and Western (B) analysis of PSII complexes. The treatments described were performed on PSII membranes; PSII complexes were then isolated by detergent treatment and column chromatography (*29*). Lanes: 1, untreated PSII; 2, PSII after salt washing to remove the 18- and 24-kDa subunits; 3, PSII after urea washing to remove MSP and other extrinsic subunits; 4, PSII after rebinding of ^{13}C-labeled MSP; 5−7, ^{13}C-labeled MSP loaded at concentrations that correspond to 1, 10, and 100% of the number of moles of MSP in lane 1. The number of moles of MSP in lane 1 was calculated assuming 2 mol of MSP (mol of reaction center)$^{-1}$ (*19*).

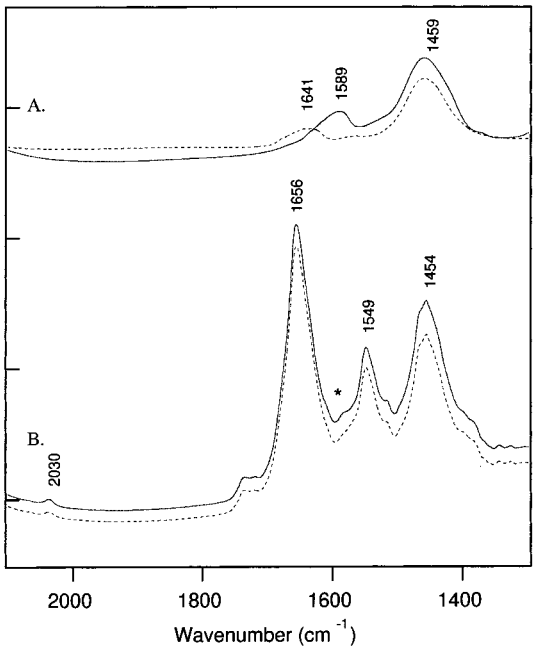

FIGURE 2: FT-IR spectra of MSP and PSII complexes. In part A, the spectra were obtained from samples containing [^{13}C]MSP in solution (solid line) and [^{12}C]MSP in solution (dashed line). Spectra were obtained at protein concentrations of 290 (solid line) and 340 μM (dashed line) and were then normalized to account for the difference in concentration. These spectra are uncorrected for differences in path length. In part B, the spectra were obtained from samples containing PSII complexes to which [^{13}C]MSP had been re-bound (solid line) and PSII complexes to which [^{12}C]MSP had been re-bound (dotted line). In part B, the line at 2030 cm^{-1} arises from the internal standard, and the asterisk marks the spectral contribution from ^{13}C-labeled MSP after reconstitution. The internal standard allows for path length correction. The marks on the *y*-axis represent increments of 0.2 AU. Spectral conditions are given in Materials and Methods.

measurements) and 1030 ± 170 μmol of O_2 (mg of Chl)$^{-1}$ h^{-1} (average of 3 measurements) for ^{12}C and ^{13}C-MSP re-bound samples, respectively. The control rate of oxygen evolution in PSII complexes, treated to deplete the 18- and 24-kDa polypeptides, was 1040 ± 50 μmol of O_2 (mg of Chl)$^{-1}$ h^{-1} (average of 3 measurements). Since these samples were subjected to chromatography in the presence of excess detergent, these experiments demonstrate that both [^{12}C]MSP and [^{13}C]MSP are bound to a high-affinity site in PSII.

In Figure 1, we present SDS−PAGE (Figure 1A) and Western analysis (Figure 1B) of such PSII complexes. In all cases, PSII membranes were the starting material, which were then treated to produce PSII complexes. Coomassie staining shows that urea treatment removes the majority of MSP (Figure 1A; compare lanes 1 and 2 with lane 3). Western analysis using an anti-MSP antibody detects bound MSP after urea treatment (Figure 1B, lane 3), but comparison to a standard curve (Figure 1B, lanes 5−7) shows that the residual MSP is a fraction of the original amount. Photosystem II complexes to which MSP has been re-bound exhibit a new band with a slightly smaller R_f when compared to native MSP (Figure 1, panels A and B, lane 4). This slower migration rate on SDS−PAGE electrophoresis is characteristic of Met-MSP (Figure 1B, lanes 5−7). As judged by both Coomassie staining and immunological detection, the content of re-bound MSP is similar to the MSP content of the control preparation (Figure 1, panels A and B; compare lanes 1 and 4).

In Figure 2A, we present FT-IR spectra of recombinant MSP derived from expression in *E. coli*. The 1900−1200 cm^{-1} region of the infrared spectrum is dominated by two vibrational lines: the amide I vibration (approximately 1650 cm^{-1}) and the amide II vibration (approximately 1550 cm^{-1}). The normal coordinate corresponding to the amide I vibration is primarily the C═O stretch of the peptide bond; the normal coordinate corresponding to the amide II vibration is predominately C−N stretch, N−H in-plane bend, and C−C stretch (*32*). Correlations of amide I, and to a lesser extent amide II, frequencies with the secondary structure of proteins in D_2O have been reported (for example, see refs *33*−*39*). D_2O exchange results in a downshift and an uncoupling of the C−N and N−H vibrational modes (*32*). Thus, the amide II vibration is observed to downshift by approximately 90−100 cm^{-1} upon deuterium exchange, and the downshifted line is referred to as the amide II′ vibration. The normal coordinate corresponding to the amide II′ vibration is complex and involves coupling between the C−N stretch, the C═O in-plane bend, and C−C stretches. The amide I′ vibration exhibits less marked changes upon deuterium exchange (*32*).

Figure 2A shows that incorporation of ^{13}C uniformly into MSP results in an overall 52 cm^{-1} downshift of the amide I′ band from 1641 to 1589 cm^{-1}. Previous analysis has shown that downshifts in the range from approximately 45 to 55 cm^{-1} are to be expected (*26, 58*). The extent of the spectral change shown here is in agreement with GC/MS estimates of the amount of ^{13}C label incorporated (>95%, data not shown). Notice that the infrared spectrum of [^{12}C]MSP (Figure 2A, dotted line) exhibits only low intensity at 1550 cm^{-1}. This line would correspond to the amide II vibration of the unexchanged peptide backbone, and low intensity in this region indicates that deuterium exchange into the protein has occurred and is extensive (*32*).

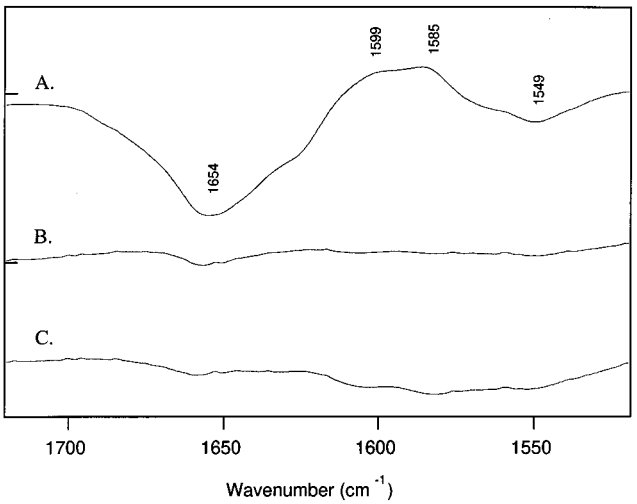

FIGURE 3: FT-IR difference spectra showing the spectral line shape of reconstituted ^{13}C-labeled MSP. In trace A, the spectrum of [^{12}C]-MSP re-bound to PSII complexes was subtracted from that of [^{13}C]-MSP re-bound to PSII complexes. In trace B, the spectrum of [^{13}C]MSP re-bound to PSII complexes was subtracted from that of [^{13}C]MSP re-bound to PSII complexes. In trace C, the spectrum of [^{12}C]MSP re-bound to PSII complexes was subtracted from that of [^{12}C]MSP re-bound toPSII complexes. An internal standard was used to ensure accurate comparison. The marks on the *y*-axis represent increments of 0.02 AU. Spectral conditions are given in Materials and Methods.

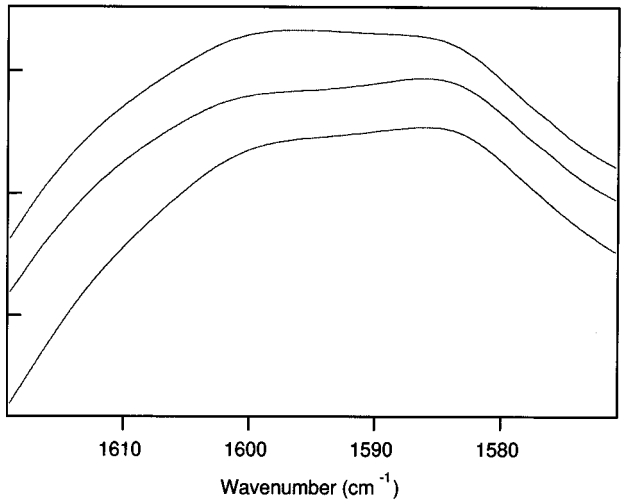

FIGURE 4: Amide I′ spectrum of the [^{13}C]MSP re-bound to PSII complexes, as derived from difference spectroscopy (see Figure 3). The three spectra demonstrate the reproducibility of the subtraction technique. The marks on the *y*-axis represent increments of 0.01 AU.

FT-IR spectra of ^{12}C and ^{13}C reconstituted MSP PSII complexes are shown in Figure 2B. Bands at 1656, 1549, and 1454 cm^{-1} correspond to the amide I′, amide II, and amide II′ vibrations, respectively (*32*). The relatively large intensity at 1549 cm^{-1} (amide II) shows that a substantial portion of PSII is resistant to deuterium exchange. Resistance to exchange in the α-helical transmembrane segments of membrane proteins has been described (*59, 60*). New intensity is observed at approximately 1600 cm^{-1} in the [^{13}C]-MSP reconstituted sample (asterisk in Figure 2B); this band has approximately the same frequency as the amide I′ band in the ^{13}C-labeled MSP sample before rebinding (compare panels A and B of Figure 2). We assign this new band to [^{13}C]MSP, which has been re-bound to the PSII reaction center.

To obtain the correct line shape for the re-bound [^{13}C]-MSP, ^{13}C-reconstituted and ^{12}C-reconstituted samples must be compared quantitatively. A spectrum of ^{12}C re-bound PSII must be subtracted from a spectrum of ^{13}C re-bound PSII (for example, Figure 2B, dashed line subtracted from solid line). Samples contained an internal standard at an invariant concentration (Figure 2B, 2030 cm^{-1}); spectra were subtracted so as to cancel the intensity at 2030 cm^{-1}. This procedure ensures the proper correction for path length differences. The amplitude of the 2030 cm^{-1} line was similar to the amplitude of the spectral feature from ^{13}C-labeled MSP. Use of the internal standard resulted in a ^{13}C minus ^{12}C difference spectrum (Figure 3) that exhibits a positive line at approximately the same frequency as [^{13}C]MSP in solution (compare Figures 3A and 2A). By contrast, use of the internal standard to subtract ^{13}C reconstituted samples from ^{13}C reconstituted samples (Figure 3B) and ^{12}C reconstituted samples from ^{12}C reconstituted samples (Figure 3C) gives the expected result, namely, a flat, featureless difference spectrum in the region from 1700 to 1500 cm^{-1}. In other regions of these difference spectra, broad lines, arising from small changes in D_2O and HDO content, prevented data interpretation.

Figure 4 shows that the spectral line shape obtained for ^{13}C-labeled and reconstituted MSP is reproducible when an internal standard is used to perform spectral subtractions. Due to spectral overlap, the line shape may be distorted from 1640 to 1620 cm^{-1} (see Figure 1A). However, there is no significant distortion expected on the low-frequency side of the [^{13}C]MSP amide I′ band. In addition to the positive band, assigned to ^{13}C-labeled MSP, the ^{13}C minus ^{12}C difference spectrum exhibits negative bands at 1654 and 1549 cm^{-1} (Figure 3A). The only contribution to this difference spectrum will be from isotope-induced shifts in MSP. Therefore, the negative band at 1654 cm^{-1} can be assigned to the expected downshift of the MSP amide I′ band upon ^{13}C labeling (Figure 3A), and the negative band at 1549 cm^{-1} is due to a ^{13}C-induced shift in the amide II band of reconstituted MSP (Figure 3A). Similar results could be obtained in the presence and absence of the internal standards, indicating that the presence of potassium ferricyanide/potassium ferrocyanide does not alter the final, re-bound conformation of MSP.

A comparison of amide I′ line shapes is presented in Figure 5. The amide I′ bands for [^{12}C]MSP, as released from PSII membranes with $CaCl_2$ and with urea, are shown in Figure 5, panels A and B, respectively. The amide I′ bands for [^{12}C]MSP and [^{13}C]MSP, as isolated from the *E. coli* expression system, are shown in Figure 5, panels C and D, respectively. Finally, Figure 5E shows the amide I′ line shape, as derived from the ^{13}C minus ^{12}C difference spectrum after rebinding of MSP to the PSII reaction center.

Dramatic spectral differences are observed among ^{12}C samples isolated from PSII membranes or from the *E. coli* expression system (Figure 5A−C). While the urea-released MSP (Figure 5B) has a broad amide I′ band, the $CaCl_2$-released MSP (Figure 5A) and [^{12}C]MSP purified from the bacterial source (Figure 5C) have relatively narrow line shapes. The shift to lower frequency when panels A and C of Figure 5 are compared is probably due to a greater extent

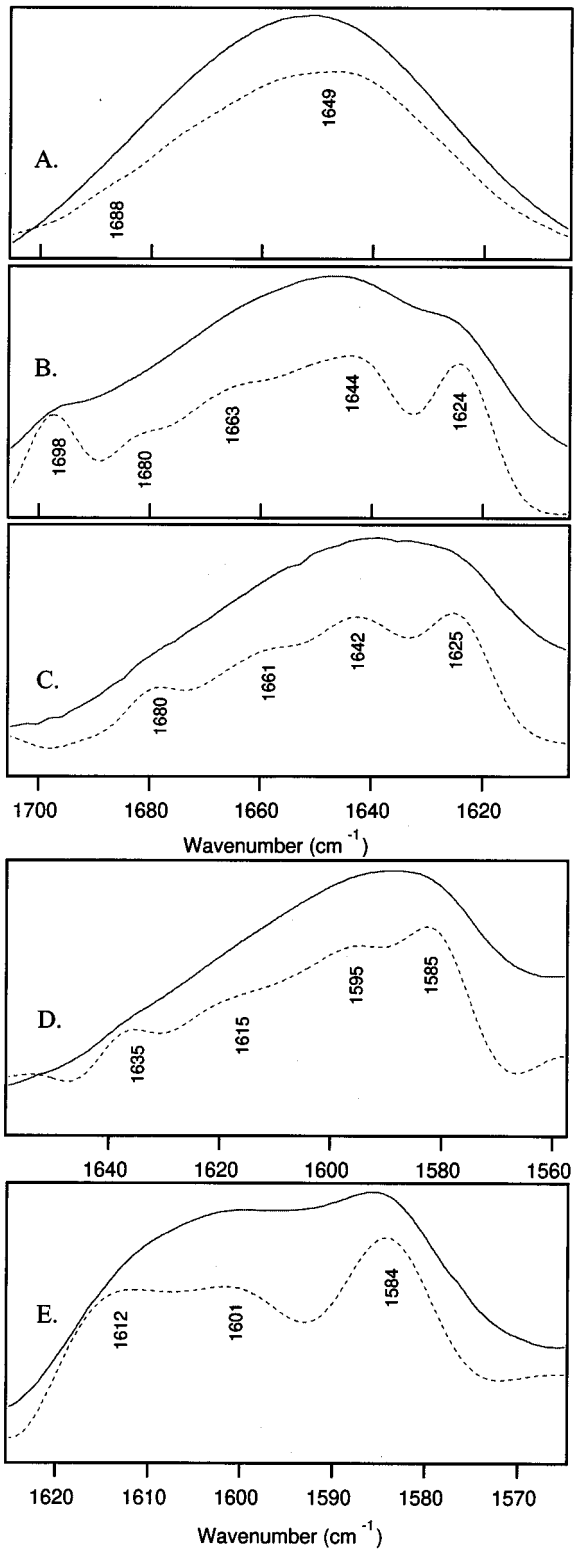

FIGURE 5: Amide I′ spectra of MSP. In all panels, the experimental spectrum is shown as a solid line and the Fourier deconvolution is shown as a dotted line. In panel A, the spectrum was obtained from MSP as isolated with $CaCl_2$ extraction of spinach PSII; in panel B, the spectrum was obtained from MSP as isolated with urea extraction of spinach PSII; in panel C, the spectrum was obtained from MSP as isolated from an expressing strain of *E. coli* grown on [^{12}C]glucose; and in panel D, the spectrum was obtained from MSP as isolated from an expressing strain of *E. coli* grown on [^{13}C]-glucose. In panel E, [^{13}C]MSP was re-bound to the PSII reaction center. The data in panel E are derived from the difference spectrum, ^{13}C minus ^{12}C (Figure 3A).

of deuterium exchange (*32*) in MSP when isolated from *E. coli.* Differences in deuterium exchange are consistent with a difference in equilibrium structure or in protein dynamics.

Differences in sample purity cannot explain these observations, since the purities of recombinant and plant MSP are similar (see Materials and Methods). The introduction of a methionine in the bacterially expressed recombinant MSP also cannot explain these observations, since such spectral differences are consistent with major changes in hydrogen bonding. The difference between [^{13}C]MSP after reconstitution and in solution cannot be ascribed to preparation-induced changes, since the samples used in these experiments were aliquots taken from the same purified preparation. Finally, note that all samples were tested and were found to rebind to PSII and to restore function, regardless of the spectral line shape obtained on any sample.

The spectral differences shown in Figure 5 represent dramatic alterations, which are evident before any spectral analysis. These data show that MSP in solution can exhibit several different infrared line shapes. A substantial alteration in amide I′ line shape was also observed upon reconstitution of [^{13}C]MSP to photosystem II. To give a more quantitative description of the nature of these alterations, band-narrowing and curve-fitting analysis were performed (reviewed in refs *30* and *31*). The amide I′ band can be considered to be a superposition of spectral components (*56*). The frequencies of these component lines are often derived from the experimental data by second-derivative (*61*) or Fourier deconvolution (*55*); these band-narrowing methods identify inflection points in the broad amide I′ line shape. This procedure identifies the number of spectral components and gives an initial frequency for each. Curve fitting then gives estimates of the contribution of each spectral component to the amide I′ band (*57*, *56*).

The dotted lines in Figure 5A−E show spectra after the application of Fourier deconvolution. The line width parameter used in Fourier deconvolution was chosen from the line widths observed in basis spectra, constructed for different secondary structural elements (*33*). The value of *K*, the resolution enhancement parameter, was chosen to be within the signal-to-noise criteria previously developed (*55*). Our rather conservative choices of *K* and the line width parameter mean that we are deriving the *minimum* number of spectral components from the data.

Comparisons of Fourier deconvolution and second-derivative spectra were used to determine the minimum number and initial positions of spectral components. Examples of such a comparison are shown in panels A and B of Figure 6. The second-derivative spectra were obtained with no spectral smoothing (*56*), and the predicted inflection points agree reasonably well with the peaks predicted from Fourier deconvolution. The relative amplitude, final frequency, and line width of each spectral component were then determined by regression analysis (*56*). We employed a nonlinear least-squares fitting procedure in which line widths, amplitudes, and peak positions of Gaussian spectral components were allowed to vary in order to minimize a reduced χ^2 parameter. This parameter is a weighted difference measure between the experimental spectrum and the line shape generated from the calculated spectral components. A converged set that accurately reproduces the spectral line shape was obtained (Figure 6 and Table 1). As examples, in Figure 6, we present

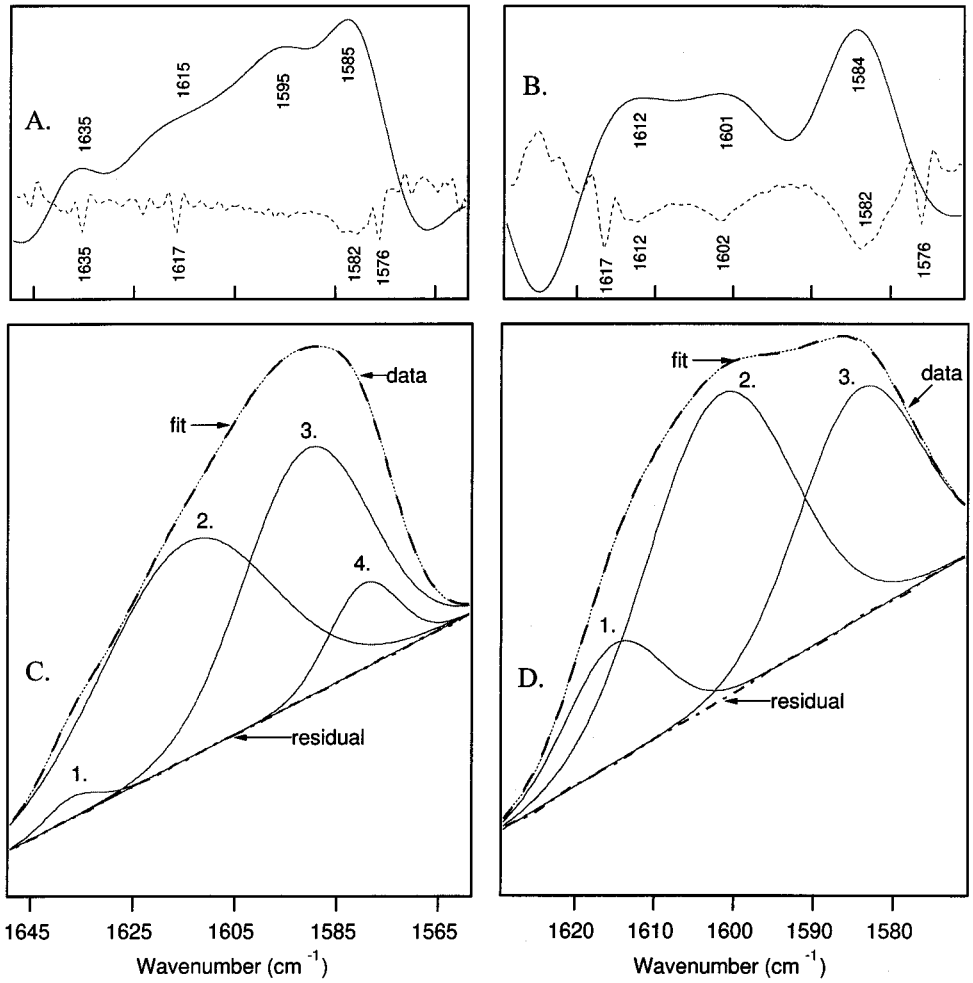

FIGURE 6: Comparison of band-narrowing (panels A and B) and nonlinear regression (panels C and D) analysis of the amide I′ band of [^{13}C]MSP in solution (panels A and C) and after rebinding to PSII complexes (panels B and D). In panels A and B, the Fourier deconvolution is shown as a solid line and the second derivative is shown as a dashed line. In panels C and D, the experimental spectrum is shown as a thin dashed line and the spectrum reconstructed after regression analysis is shown as a thick dashed line. The spectral components employed are the numbered Gaussians, and the residual obtained is shown.

the results of such an analysis on [^{13}C]MSP in solution (Figure 6A,C) and after rebinding of [^{13}C]MSP to PSII (Figure 6B,D). In each panel, the data are shown in the thin dotted line, and the predicted line shape obtained from the spectral components shown (Figure 6, numbered peaks 1−4 in panel C and 1−3 in panel D) is represented in the thick dashed line. The final agreement between the experimental data and the fit is good, as judged by the residual (Figure 6C,D) and reduced χ^2 parameters (data not shown).

Nonlinear least-squares analysis was also performed with fixed frequencies, as derived from Fourier deconvolution. Iterative alterations in only bandwidth and amplitude were permitted. This procedure was found to give a less accurate fit to the observed spectral line shape, as judged by the residual and the reduced χ^2 parameter (data not shown).

The contribution of each spectral component to the total area under the amide I′ band is summarized in Table 1. This information is given for [^{13}C]MSP in solution and after rebinding (Figure 6C,D), as well as for the [^{12}C]MSP protein in solution (Figure 5A−C). Upon reconstitution, [^{13}C]MSP exhibits a decrease in the contribution from a spectral component at 1615 cm^{-1}, an increase in a spectral component at 1584 cm^{-1}, and a new spectral component at 1602 cm^{-1} (Table 1). The spectral region from 1640 to 1620 cm^{-1} is not interpretable in this spectrum because of spectral overlap. A spectral component at 1590 cm^{-1} that makes a large contribution to the solution [^{13}C]MSP spectrum is not observed upon rebinding. If one ignores the possible effects of transition dipole coupling (*32, 62*), then the overall downshift observed in major spectral components upon rebinding of [^{13}C]MSP to the reaction center is consistent with an increase either in the number of hydrogen bonds or in the strength of existing hydrogen bonds.

Since the spectral region from 1640 to 1620 cm^{-1} could not be used in analysis of the re-bound [^{13}C]MSP spectrum, the percentages obtained (Table 1) are overestimates of the contribution of each spectral component to the overall line shape. However, we estimate that the correction is small (less than 5%) on the basis of the observed small contribution of spectral components in this region to other MSP spectra and on the basis of an extrapolation of the quality of the fit at 1630 cm^{-1} (see the spectrum of re-bound [^{13}C]MSP, Figure 6D). An approximately 5% correction would not change the conclusions of our study (Table 1).

^{13}C labeling has the effect of shifting all spectral components approximately equally (*26, 58*). The average shift for MSP is 52 cm^{-1} (Figure 1A). Table 1 shows adjustments of the frequencies of spectral components (Figure 5D,E) for

Table 1: Results of Regression Analysis of the Amide I′ Band of MSP

spectrum	cm^{-1} [a]	adj. cm^{-1} [b]	% total area
$CaCl_2$-isolated MSP, soln	1648		75
	1681		25
urea-isolated MSP, soln	1624		8
	1641		3
	1653		72
	1690		15
	1698		2
^{12}C MSP, soln	1627		37
	1643		12
	1657		43
	1679		8
^{13}C MSP, soln	1580	1632	6
	1590	1642	44
	1615	1667	49
	1637	1689	1
^{13}C MSP, re-bound	1584	1636	32
	1602	1654	55
	1615	1667	13
	1637	NA	NA

[a] Frequency of the spectral component derived from the regression analysis of the experimental data. The number of spectral components and the initial estimates of the frequency were derived from Fourier deconvolution and the second-derivative spectrum. The frequencies, amplitudes, and line widths were varied in the regression analysis. The resulting spectral components are shown here. Examples of the qualities of the fits are shown in Figure 6. [b] Frequency adjusted for the average 52-cm^{-1} downshift observed upon ^{13}C labeling.

this 52 cm^{-1} downshift. This adjustment facilitates a comparison of spectra of [^{13}C]MSP with data obtained on [^{12}C]MSP, as expressed in *E. coli* or as isolated from spinach PSII.

The solution structure of the [^{12}C]MSP isolated from *E. coli* was also analyzed (Table 1). Major spectral components at 1627 (37%) and 1657 cm^{-1} (43%) are observed. The spectrum exhibits minor components at 1643 and 1679 cm^{-1}. Observed changes when [^{12}C]MSP and [^{13}C]MSP are compared are not likely to be due to an isotope effect on the structure of MSP, since the magnitude of a ^{13}C-induced effect should be small (*63*). These data show that the structures of [^{12}C]MSP and [^{13}C]MSP in solution are not the same. Significant differences are also observed between the solution structures of [^{12}C]MSP isolated from PSII and [^{12}C]MSP expressed in *E. coli* (Table 1). We conclude that, in solution, MSP can sample a variety of conformational states, which differ in hydrogen bonding of the peptide backbone. Some of the accessible conformations in solution may have secondary structural contents that are similar to that of rebound MSP.

DISCUSSION

Spectral components in the amide I band are often assigned to specific types of secondary structure elements (reviewed in refs *30* and *31*). These assignments have been developed and are based on studies of proteins with known structures (for example, see ref *57*). These studies are often performed in D_2O to avoid the contribution of H_2O in the amide I region (discussed in ref *35*). Due to overlap of spectral ranges, some secondary structure assignments are not unique.

Assumptions Employed in Quantitative Analysis of Amide I Line Shapes. The method that we have used for quantitative prediction makes three assumptions. First, this method assumes that the molar absorptivities of different secondary structural elements are similar. This idea has been evaluated, and the molar absorptivities have been found to be within a factor of 1.5, at least for protein films (*64*). Second, this method assumes that side-chain contributions in the amide I region are minimal. Although controversial (*30, 31*), there is some experimental support for this idea (*33*). Third, this method relies on assignments based on a database of proteins with known X-ray structures (*56*). Since extrinsic subunits of membrane proteins are not represented in this data base, application of this method necessitates the assumption that secondary structural elements in MSP will be similar to those found in other globular proteins. This seems a reasonable assumption at present. Linear algebraic methods of amide I band analysis, such as singular value decomposition and factor analysis, have also been applied to the prediction of secondary structure (*33*−*35, 37*−*39*). The advantages and disadvantages of these approaches have also been discussed (*30, 31*). Given the fact that methods of quantitative prediction of secondary structure from infrared data are still under development, we stress the qualitative conclusions of our study and do not rely on the exact percentages derived from the curve-fitting analysis. The spectroscopic alterations, from which we deduce these structural changes, are substantial and are evident from the experimental data before the application of band-narrowing analysis.

Assignment of Spectral Components to Secondary Structural Elements. Infrared analysis is most reliable in the assignment of spectral components between 1630 and 1620 cm^{-1} to β-sheet (*33, 36, 30*). High-frequency components (1670−1690 cm^{-1}) of lower intensity have also been assigned to β-sheet; the two components are derived from transition dipole coupling (*32*). When proteins contain mainly β-sheet, a maximum at approximately 1634 cm^{-1} and a strong shoulder at 1660 cm^{-1} are observed (*33*). These spectral components have been assigned to turns of the protein backbone (*30, 31*). For example, immunoglobulin G, a β-sheet protein, exhibits such a 1660 cm^{-1} spectral component and a maximum at 1638 cm^{-1} (data not shown). Although a potential contribution in the 1630−1620 cm^{-1} region from α-helix has been identified in model calculations (*62*), such a contribution can be distinguished from the spectra of β-sheets, since the α-helical structure will be accompanied by an intense spectral component at 1650 cm^{-1}. This is the assignment most often associated with an α-helix (*57, 65*).

Infrared spectroscopy is not as reliable an indicator of α-helical content, since turns or loops (*36, 66*) can contribute in the spectral region near 1650 cm^{-1}. Contributions near 1640 cm^{-1} are often assigned to random conformations in proteins. In this context, "random" can indicate either conformational mobility or irregularity in secondary structure (*30, 31*). Some studies find a contribution at approximately 1640 cm^{-1} from 3_{10}-helix in proteins (*67*−*69*), although this assignment is controversial (*70, 71*).

Conclusions from Spectral Data Obtained upon Rebinding of [^{13}C]MSP. Given the ambiguities associated with the use of these assignments at this time, we will employ this information in a conservative fashion. In the analysis below, we add the average ^{13}C shift, 52 cm^{-1} (see Figure 2A), to the spectral components derived from the line shapes of ^{13}C-labeled MSP; this facilitates comparison with spectral ranges

derived for ^{12}C proteins. We compare [^{13}C]MSP in solution with [^{13}C]MSP after rebinding, because these samples were different aliquots of the same preparation and should be directly comparable.

An increase in amplitude is observed at 1584 cm^{-1} (1636 cm^{-1} if ^{12}C) when [^{13}C]MSP binds to the PSII reaction center. On the basis of the considerations described above, we assign this alteration to a substantial increase (26%) in the content of β-sheet upon rebinding. A decrease in amplitude is observed in spectral components at 1590 cm^{-1} (1642 cm^{-1} if ^{12}C) and 1615 cm^{-1} (1667 cm^{-1} if ^{12}C) when [^{13}C]MSP binds to the PSII reaction center. On the basis of previous studies of proteins in D_2O buffers, these spectral components can be assigned to random structures and to turns. The change in both spectral components simultaneously supports this assignment, rather than an assignment to 3_{10}-helix, although this latter possibility cannot be absolutely excluded. The increase in amplitude at 1602 cm^{-1} (1654 cm^{-1} if ^{12}C) when [^{13}C]MSP binds to the PSII reaction center is also significant, but unfortunately, assignments in this spectral region are not well defined. This spectral change may be due to an increase in α-helical or loop content.

This interpretation of our infrared spectra leads to the conclusion that the change in amide I line shape when [^{13}C]-MSP binds to the reaction center is consistent with an increase in the proportion of β-sheet and a decrease in random structure. Overall, approximately 30−40% of the peptide backbone undergoes a change in hydrogen bonding (Table 1). The increase in β-sheet content upon rebinding of MSP to the PSII reaction center implies that MSP interacts with PSII through extended strand domains and that reconstitution induces folding of MSP. The structure of bound MSP is interpreted as the physiologically relevant conformation, since binding of MSP restores oxygen evolution to PSII and since the re-bound structure is reproducible.

The method employed above assumes that the ^{13}C-induced shifts of the C═O vibration are equal for each secondary structural element. This assumption is supported by the literature (see ref *26*, but see also ref *58*). An alternate method of correction would be to obtain an estimate of the magnitude of the ^{13}C shifts for each spectral component by comparison of [^{12}C]MSP and [^{13}C]MSP in solution. However, we feel that this is an unreliable correction protocol because of the structural heterogeneity observed for MSP in solution. Also, it should be noted that in a previous study (*58*), when a range of ^{13}C shifts was observed, the range of observed values was 49 ± 6 cm^{-1}, compared to the overall average shift of 55 cm^{-1} observed in that work (*58*). Similar, small changes in the magnitude of ^{13}C shifts for different secondary structural elements would not change the conclusions of our study, since we are comparing the conformation of ^{13}C-labeled MSP in solution with the conformation of ^{13}C-labeled MSP after rebinding.

Conclusions from Spectral Data Obtained on [^{13}C]MSP and [^{12}C]MSP in Solution. Our results have also provided spectroscopic evidence for considerable variation in the solution structure of MSP. By application of the same methods of analysis to MSP in solution, the data support the conclusion that the content of β-sheet, random structure, turns, and possibly helix varies dramatically among MSP preparations, all of which are capable of rebinding to PSII and restoring function to the active site. We conclude that, in solution, MSP can sample a range of shallow energy minima, each of which is defined by a difference in hydrogen bonding of the peptide backbone. Some of the solution-accessible structures may be similar to that of re-bound MSP.

Our conclusion that MSP lacks a well-defined structure in solution is supported by the infrared spectroscopy literature. The amide I line shapes reported for MSP in solution exhibit considerable variation from study to study (*40*−*43*, *52*). Also, while amide I line shape changes have been attributed to addition of metals (*43*), we see an equivalent or greater amount of variation without addition of metal ions. In one recent report, a dramatically altered amide I line shape, with a maximum at approximately 1620 cm^{-1}, has been reported after lyophilization of MSP (*43*). This line shape may be due to aggregation of the protein after freeze−drying, which promotes intermolecular hydrogen bonding (*72*). Such intermolecular hydrogen bonding gives rise to spectral components at frequencies of approximately 1620−1610 cm^{-1}.

The observation of substantial conformational heterogeneity in solution MSP may seem unusual, given the fact that the structures of globular proteins are usually considered to be well defined and unique. However, MSP may be a new member of a class of proteins referred to as natively unfolded (*73*). Like MSP, natively unfolded proteins are acidic proteins involved in protein−protein interactions. This class of proteins is characterized by anomalous hydrodynamic behavior and a significant amount of random structure in solution (*73*). It has been speculated that conformational heterogeneity in solution may be important in facilitating the binding of natively unfolded proteins to their protein targets (*73*).

Secondary Structural Models for MSP Can Be Used To Rationalize the Conformational Heterogeneity Observed for MSP in Solution. Models for the secondary structure of MSP have been derived (*52*, *74*). The models agree in the prediction of a substantial amount of β-sheet (33−38%). Each model predicts that the primary sequence through some of the putative β-strands is primarily hydrophobic. β-Strands in water-soluble proteins usually exhibit alternating hydrophilic and hydrophobic amino acid side chains. Such a primary structure gives a β-sheet with one hydrophobic and one hydrophilic face; this structure facilitates the stability of globular proteins. The increase in β-structure upon rebinding of MSP to PSII and the differences in secondary structure observed for solution MSP suggest not only that MSP binds to PSII through β-strands but also that these unusual repeated (rather than alternating) hydrophobic structural elements may be responsible for destabilizing the protein in solution.

Previous Results from Circular Dichroism Studies. Circular dichroism can also be used to predict secondary structure in proteins. While considerable variation exists in the literature as far as infrared spectra of MSP, the CD spectra of MSP are in reasonable agreement (*52*, *74*). This is an interesting observation, which may have its basis in the physical basis of the two types of spectroscopy. While CD is sensitive to long-range chiral structure in proteins, FT-IR spectroscopy is sensitive to short-range hydrogen bonding and nonbonding interactions. We will explore this issue in future work.

General Conclusions. Our findings of substantial alterations in the secondary structure of MSP upon interaction with the reaction center may have implications for the assembly of other multi-subunit membrane proteins. There is little information currently available about the mechanism of such assembly. The system employed here is advantageous in that a functional assay exists for binding of the extrinsic subunit. Our results suggest that the reaction center acts as a template upon which the extrinsic subunit, MSP, folds and attains its final structure.

ACKNOWLEDGMENT

The authors thank R. Boyle and D. Lu for technical support and Dr. Sunyoung Kim for helpful discussions. We acknowledge the Imaging Center in the College of Biological Sciences and T. Krick in the University of Minnesota Mass Spectrometry Facility (Agriculture Experiment Station).

REFERENCES

1. Yocum, C. F. (1992) in *Manganese Redox Enzymes* (Pecoraro, V. L., Ed.) pp 71−83, VCH Publishers, New York.
2. Barry, B. A., Boerner, R. J., and de Paula, J. C. (1994) in *The Molecular Biology of the Cyanobacteria* (Bryant, D., Ed.) pp 215−257, Kluwer Academic Publishers, Dordrecht.
3. Oh-oka, H., Tanaka, S., Wada, K., Kuwabara, T., and Murata, N. (1986) *FEBS Lett. 197*, 63−66.
4. Erickson, J. M., and Rochaix, J.-D. (1992) in *The Photosystems: Structure, Function, and Molecular Biology* (Barber, J., Ed.) pp 101−177, Elsevier, Amsterdam.
5. Xu, Q., and Bricker, T. M. (1993) *J. Biol. Chem. 267*, 25816−25821.
6. Miyao, M., and Murata, N. (1989) *Biochim. Biophys. Acta 977*, 315−321.
7. Leuschner, C., and Bricker, T. M. (1996) *Biochemistry 35*, 4551−4557.
8. Bockholt, R., Masepohl, B., and Pistorius, E. K. (1991) *FEBS Lett. 294*, 59−63.
9. Burnap, R. L., and Sherman, L. A. (1991) *Biochemistry 30*, 440−446.
10. Mayes, S. R., Cook, K. M., Self, S. J., Zhang, Z., and Barber, J. (1991) *Biochim. Biophys. Acta 1060*, 1−12.
11. Philbrick, J. B., Diner, B. A., and Zilinskas, B. A. (1991) *J. Biol. Chem. 266*, 13370−13376.
12. Vass, I., Cook, K. M., Deak, Z., Mayes, S. R., and Barber, J. (1992) *Biochim. Biophys. Acta 1102*, 195−201.
13. Mayfield, S. P., Bennoun, P., and Rochaix, J.-D. (1987) *EMBO J. 6*, 313−318.
14. Akerlund, H.-E., and Jansson, C. (1981) *FEBS Lett. 124*, 229−232.
15. Yamomoto, Y., Doi, M., Tamura, N., and Nishimura, N. (1981) *FEBS Lett. 133*, 265−268.
16. Ono, T., and Inoue, Y. (1983) *FEBS Lett. 164*, 252−260.
17. Miyao, M., and Murata, N. (1984) *FEBS Lett. 170*, 350−354.
18. Miyao, M., and Murata, N. (1983) *FEBS Lett. 164*, 375−378.
19. Bricker, T. M. (1992) *Biochemistry 31*, 4623−4628.
20. Betts, S. D., Hachigian, T. M., Pichersky, E., and Yocum, C. F. (1994) *Plant Mol. Biol. 26*, 117−130.
21. Ono, T., and Inoue, Y. (1984) *FEBS Lett. 168*, 281−286.
22. Miyao, M., Murata, N., Lavorel, J., Maison-Peteri, B., Boussac, A., and Etienne, A.- L. (1987) *Biochim. Biophys. Acta 890*, 151−159.
23. Vass, I., Ono, T., and Inoue, Y. (1987) *Biochim. Biophys. Acta 892*, 224−235.
24. Burnap, R. L., Shen, J.-R., Jursinic, P. A., Inoue, Y., and Sherman, L. A. (1992) *Biochemistry 31*, 7404−7410.
25. Seidler, A., and Michel, H. (1990) *EMBO J. 9*, 1743−1748.
26. Haris, P. I., Robillard, G. T., van Dijk, A. A., and Chapman, D. (1992) *Biochemistry 31*, 6279−6284.
27. van Nuland, N. A. J., van Duk, A. A., Dijkstra, K., van Hoesel, F. H. J., Sheek, R. M., and Robillard, G. T. (1992) *Eur. J. Biochem. 203*, 483−491.
28. Berthold, D. A., Babcock, G. T., and Yocum, C. F. (1981) *FEBS Lett. 134*, 231−234.
29. MacDonald, G. M., and Barry, B. A. (1992) *Biochemistry 31*, 9848−9856.
30. Surewicz, W. K., Mantsch, H. A., and Chapman, D. (1993) *Biochemistry 32*, 389−394.
31. Jackson, M., and Mantsch, H. H. (1995) *Crit. Rev. Biochem. Mol. Biol. 30*, 95−120.
32. Krimm, S., and Bandekar, J. (1986) in *Advances in Protein Chemistry* (Anfinsen, C. B., Edsall, J. T., and Richards, F. M., Eds.) pp 181−364, Academic Press, New York.
33. Eckert, K., Grosse, R., Malur, J., and Repke, K. R. H. (1977) *Biopolymers 16*, 2549−2563.
34. Dousseau, F., and Pezolet, M. (1990) *Biochemistry 29*, 8771−8779.
35. Lee, D. C., Haris, P. I., Chapman, D., and Mitchell, R. C. (1990) *Biochemistry 29*, 9185−9193.
36. Prestrelski, S. J., Byler, D. M., and Liebman, M. N. (1991) *Biochemistry 30*, 133−143.
37. Sarver, R. W., and Krueger, W. C. (1991) *Anal. Biochem. 194*, 89−100.
38. Pribic, R., van Stokkum, I. H. M., Chapman, D., Haris, P. I., and Bloemendal, M. (1993) *Anal. Biochem. 214*, 366−378.
39. Rahmelow, K., and Hubner, W. (1996) *Anal. Biochem. 241*, 5−13.
40. Ahmed, A., Tajmir-Riahi, H. A., and Carpentier, R. (1995) *FEBS Lett. 363*, 65−68.
41. Zhang, H. M., Fischer, G., and Wydrzynski, T. (1995) in *Photosynthesis: from Light to Biosphere* (Mathis, P., Ed.) pp 447−450, Kluwer Academic Press, Amsterdam.
42. Sonoyama, M., Motoki, A., Okamoto, G., Hirano, M., Ishida, H., and Katoh, S. (1996) *Biochim. Biophys. Acta 1297*, 167−170.
43. Zhang, L.-X., Liang, H.-G., Wang, J., Li, W.-R., and Yu, T.-Z. (1996) *Photosynth. Res. 48*, 379−384.
44. Betts, S. D., Ross, J. R., Hall, K. U., Pichersky, E., and Yocum, C. F. (1996) *Biochim. Biophys. Acta 1274*, 135−142.
45. Betts, S. D., Ross, J. R., Pichersky, E., and Yocum, C. F. (1996) *Biochemistry 35*, 6302−6307.
46. Kuwabara, T., Murata, T., Miyao, M., and Murata, N. (1986) *Biochim. Biophys. Acta 850*, 146−155.
47. Miyao, M., and Murata, N. (1983) *Biochim. Biophys. Acta 725*, 87−93.
48. Fersht, A. (1977) *Enzyme structure and mechanism*, p 170, W. H. Freeman and Co., New York.
49. Patterson, B. W., Carraro, F., and Wolfe, R. R. (1993) *Biol. Mass Spectrosc. 22*, 518−523.
50. Lichtenthaler, H. K. (1987) *Methods Enzymol. 148*, 350−382.
51. Barry, B. A. (1995) *Methods Enzymol. 258*, 303−319.
52. Xu, Q., Nelson, J., and Bricker, T. M. (1994) *Biochim. Biophys. Acta 1188*, 427−431.
53. Piccioni, R., Bellemare, G., and Chua, N. (1982) in *Methods in Chloroplast Molecular Biology* (Edelman, H., Hallick, R. B., and Chua, N.-H., Eds.) pp 985−1014, Elsevier, Amsterdam.
54. Noren, G. H., Boerner, R. J., and Barry, B. A. (1991) *Biochemistry 30*, 3943−3950.
55. Kauppinen, J. K., Moffatt, D. J., Mantsch, H. H., and Cameron, D. G. (1981) *Appl. Spectrosc. 35*, 271−276.
56. Susi, H., and Byler, D. M. (1986) *Methods Enzymol. 130*, 290−311.
57. Byler, D. M., and Susi, H. (1986) *Biopolymers 25*, 469−487.
58. Zhang, M., Fabian, H., Mantsch, H. H., and Vogel, H. J. (1994) *Biochemistry 33*, 10883−10888.
59. Earnest, T. N., Herzfeld, J., and Rothschild, K. J. (1990) *Biophys. J. 58*, 1539−1546.
60. Bernard, M. T., MacDonald, G. M., Nguyen, A. P., Debus, R. J., and Barry, B. A. (1995) *J. Biol. Chem. 270*, 1589−1594.
61. Dong, A., Huang, P., and Caughey, W. S. (1990) *Biochemistry 29*, 3303−3308.

62. Torii, H., and Tasumi, M. (1992) *J. Chem. Phys. 96*, 3379−3387.
63. Schowen, K. B., and Schowen, R. L. (1982) *Methods Enzymol. 87*, 551−606.
64. de Jongh, H. H. J., Goormaghtigh, E., and Ruysschaert, J.-M. (1996) *Anal. Biochem. 242*, 95−103.
65. Surewicz, W. K., and Mantsch, H. H. (1988) *Biochim. Biophys. Acta 952*, 115−130.
66. Wilder, C. L., Friedrich, A. D., Potts, R. O., Daumy, G. O., and Francoeur, M. L. (1992) *Biochemistry 31*, 27−31.
67. Holloway, P. W., and Mantsch, H. H. (1988) *Biochemistry 28*, 931−935.
68. Prestrelski, S. J., Byler, D. M., and Thompson, M. P. (1991) *Int. J. Pept. Protein Res. 57*, 508−512.
69. Fabian, H., Naumann, D., Misselwitz, R., Ristau, O., Gerlach, D., and Welfle, H. (1992) *Biochemistry 31*, 6532−6538.
70. Yasui, S. C., Keiderling, T. A., Bonora, G. M., and Toniolo, C. (1986) *Biopolymers 25*, 79−89.
71. Kennedy, D. F., Crisma, M., Toniolo, C., and Chapman, D. (1991) *Biochemistry 30*, 6541−6548.
72. Clark, A. H., Saunderson, D., and Suggett, A. (1981) *Int. J. Pept. Protein Res. 17*, 353−364.
73. Weinreb, P. H., Zhen, W., Poon, A. W., Conway, K. A., and Lansbury, P. T., Jr. (1996) *Biochemistry 35*, 13709−13715.
74. Shutova, T., Irrgang, K.-D., Shubin, V., Klimov, V. V., and Renger, G. (1997) *Biochemistry 36*, 6350−6358.
75. Betts, S. (1995) Ph.D. Thesis, University of Michigan.

BI9724467